Theory and Design of a *Ku*-Band TE_{21}-Mode Coupler

YOUN H. CHOUNG, MEMBER, IEEE, KENNETH R. GOUDEY, AND LAWRENCE G. BRYANS, MEMBER, IEEE

***Abstract*—This paper describes a TE_{21}-mode tracking coupler for satellite earth stations communications antennas which require autotrack capability. The paper covers theoretical coupler designs as well as laboratory test results from *Ku*-band hardware.**

I. Introduction

SINCE THE ADVENT of satellite communications, large ground-station antennas with narrow microwave beams have been used to communicate with satellites. In order to point these narrow beams at the satellite, various tracking methods have been employed. The most accurate of these methods uses a pattern having a null in the direction of the communications beam peak which is compared to the communications or sum pattern to yield a tracking error signal. This pattern is called a difference pattern and may be generated in the antenna feed using waveguide modes such as the TE_{21} mode in circular waveguide in addition to the TE_{11} mode used for communication. A diagram of a typical antenna feed employing TE_{21}-mode tracking and TE_{11} communications modes is shown in Fig. 1.

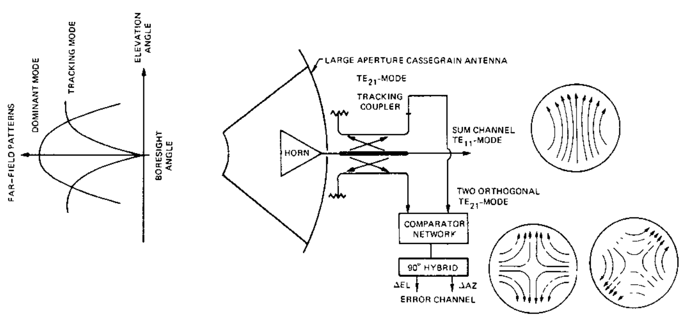

Fig. 1. Tracking feed system.

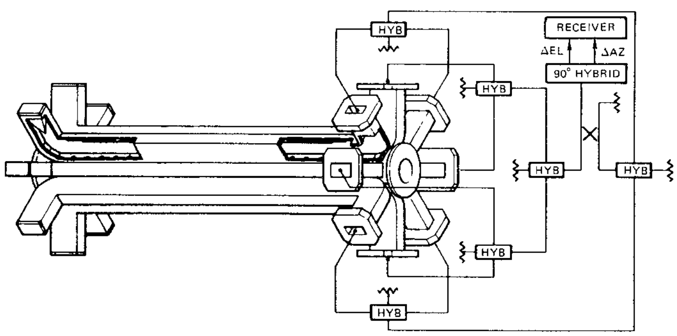

Fig. 2. Layout of TE_{21}-mode coupler using two orthogonal modes.

With the boresight axis defined as the direction to the satellite, the main or sum beam axis is colinear with the boresight axis when only the dominant mode is excited at the aperture of the feed. When the main beam axis is not aligned with the boresight axis, higher order modes are excited in the feed. The amplitude of the higher TE_{21} mode is proportional to the angle of misalignment. In practice, when an incoming wave is received by the antenna, the output level of the communication signal yields a "sum" voltage, while an "error" voltage is generated corresponding to the angular error of the antenna when its pointing direction deviates from the source direction. The sum-channel and error-channel signals are supplied to a tracking receiver which in turn drives the antenna to boresight through an antenna servo system.

The overall layout of a coupler using two orthogonal TE_{21} modes is shown in Fig. 2. Four coupling arms are summed through a network to obtain a single TE_{21}-mode coupler. The two TE_{21}-mode couplers are then summed together through a final 90° hybrid to separate the azimuth and elevation error signals.

II. Design Theory

Theoretical design of the TE_{21} coupler was done by using "loose" and "tight" coupled-mode theory. Loose coupling theory [1], [2] shows how to taper coupling to minimize the length of the coupling region, while tight coupling theory [1], [2] defines the periodic exchange of energy between coupled waves. The design procedure calls for first finding the desired coupling taper distribution $\phi(x)$ for minimization of coupling to undesired modes by neglecting the transferred power between the coupled waves, and secondly considering the power transferred to the desired TE_{21} mode.

A. Loose Coupling Theory

A general circuit diagram of coupled transmission lines is shown in Fig. 3. Coupling between the lines may be defined as the ratio of the forward current for $\beta_1 \neq \beta_2$ to

Manuscript received February 19, 1982; revised April 28, 1982.
The authors are with the Ford Aerospace and Communications Corp., 3939 Fabian Way, Palo Alto, CA 94303.

0018-9480/82/1100-1862$00.75 ©1982 IEEE

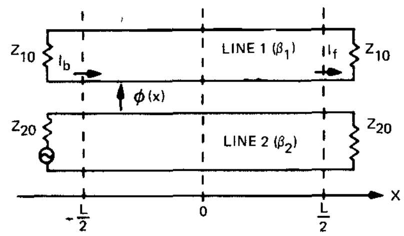

Fig. 3. Circuit diagram of coupled transmission lines.

the forward current for $\beta_1 = \beta_2$. Directivity may be defined as the ratio of the backward current for $\beta_1 \neq \beta_2$ to the forward current for $\beta_1 = \beta_2$

$$\text{Coupling} = \left| \frac{I_f(\beta_1 \neq \beta_2)}{I_f(\beta_1 = \beta_2)} \right| = \frac{\int_{-L/2}^{L/2} \phi(x) e^{-j(2\pi/L)\theta_c x}\, dx}{\int_{-L/2}^{L/2} \phi(x)\, dx}$$

$$\text{Directivity} = \left| \frac{I_b(\beta_1 \neq \beta_2)}{I_f(\beta_1 = \beta_2)} \right| = \frac{\int_{-L/2}^{L/2} \phi(x) e^{-j(2\pi/L)\theta_D x}\, dx}{\int_{-L/2}^{L/2} \phi(x)\, dx} \tag{1}$$

where

$$\theta_{C_D} = \frac{L}{2\pi}(\beta_1 \mp \beta_2),$$

$$\theta_C = \text{coupling parameter}, \qquad \theta_D = \text{directivity parameter} \tag{2}$$

- β_1 phase constant of line 1 for the particular mode considered,
- β_2 phase constant of line 2 for the particular mode considered,
- L length of the coupling section,
- $\phi(x)$ coupling function. More precisely, $1/\phi(x)$ is the ratio of the voltage on line 2 to the voltage on line 1 at x [1].

For the TE_{21}-mode coupler, line 1 is a circular waveguide and line 2 is a rectangular waveguide. $\phi(x)$ results from a coupling structure on the common wall between the two waveguides composed of an array of coupling holes. Each coupling hole may be considered a discrete coupling point. Let $\phi_i(X)$ be a known coupling function for the ith coupling point and F_i be the finite Fourier transform of $\phi_i(X)$

$$F_i(\theta) = \int_{-L/2}^{L/2} \phi_i(X) e^{-j(2\pi/L)\theta X}\, dX. \tag{3}$$

Consider the case of tapered amplitudes and an even number ($2N$) of equally spaced couplings. Let a_i be the coupling strengths and s be the spacing between coupling points. Then $\phi(X)$ is expressed as

$$\phi_i(x) = \begin{cases} a_i & \text{at } x = \pm \frac{S}{2}(2i-1), \quad i = 1,2,\cdots,N \\ 0 & \text{otherwise} \end{cases} \tag{4}$$

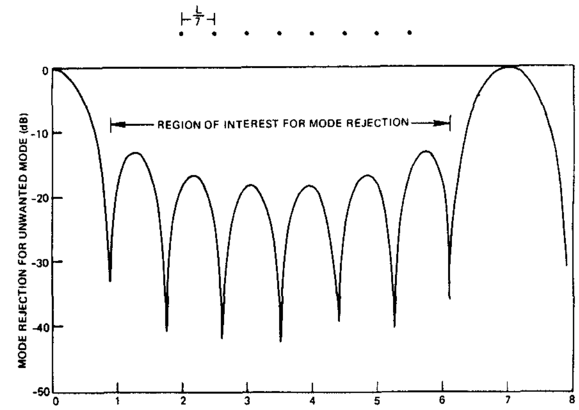

Fig. 4. Directivity of 8 equal-strength equally spaced coupling points.

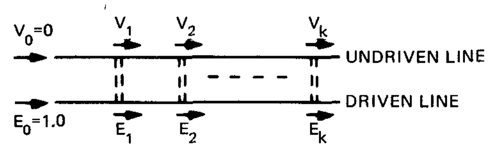

Fig. 5. Transmission lines with multiple point couplings.

The transform for the total coupling distribution is

$$F_{C_D} = 2\sum_{i=1}^{N} a_i \cos\left[\frac{S}{2}(\beta_1 \mp \beta_2)\right] = 2\sum_{i=1}^{N} a_i \cos\left(\frac{2i-1}{2N-1}\pi\theta_{C_D}\right). \tag{5}$$

Therefore, the coupling and the directivity can be defined as

$$\begin{bmatrix}\text{Coupling}\\ \text{Directivity}\end{bmatrix} = \frac{F_{C_D}}{F_{C_D}(\theta = 0)} = \frac{\sum_{i=1}^{N} a_i \cos\left(\frac{2i-1}{2N-1}\pi\theta_{C_D}\right)}{\sum_{i=1}^{N} a_i}. \tag{6}$$

This mode coupler design method optimizes the number of coupling points to meet required coupling and directivity levels. For example, consider mode rejection (coupling or directivity) for uniform coupling with 8 equally spaced points ($N = 4$ and a_i = constant) which is plotted in Fig. 4. For the tracking mode coupler design developed, the region of interest for 8 coupling points is $0.9 < \theta < 6.1$. This design results in only 13-dB rejection of the unwanted mode. This result indicates that either the coupling distribution should be modified or the number of coupling holes should be increased or both to obtain a desired 40-dB rejection. To accomplish this rejection, the actual coupler design was derived from a modified distribution where 32-, 48-, or 64-point couplings were considered.

B. Tight Coupling Effects of Multiple Discrete Couplings

Assume that two transmission lines have identical propagation constants with coupling units located at intervals along the lines shown in Fig. 5. If m_i couplings of magnitude α_i are located along the lines in any order, the wave amplitudes in the driven and undriven lines are [1]

$$E = \cos\left(\sum_{i=1}^{K} m_i \sin^{-1}\alpha_i\right), \qquad \text{driven} \tag{7}$$

$$V = \sin\left(\sum_{i=1}^{K} m_i \sin^{-1}\alpha_i\right), \qquad \text{undriven.} \tag{8}$$

Our case is symmetric, equally spaced, and has an even number of points ($2N$). This means that $m_i = 2$ and the summation extends over N. Let

$$\alpha_i = a_i \alpha_0 \tag{9}$$

where α_0 is the coupling magnitude of the reference point and a_i is the coupling distribution ratio with respect to the reference point. Then the coupling ratio V/E can be expressed as

$$\frac{V}{E} = \tan\left[2\sum_{i=1}^{N} \sin^{-1}(a_i\alpha_0)\right]. \tag{10}$$

Given α_0, the coupling ratio V/E is determined, since the a_i distribution is an input parameter describing the required coupling from loose coupling theory and the selected $\phi(X)$ distribution.

V/E measures coupling for the desired mode and shows a cyclical energy transfer between coupled waves. F_c is a loose coupling for mode rejection when the transferred power between the two lines is negligible, and is uniform for the desired mode assuming 100 percent coupling. Therefore, F_c is used for the mode rejection and V/E is used for the desired mode coupling.

III. *Ku*-Band TE_{21}^C-Mode Coupler Design

The design goal was to generate TE_{21}^C from TE_{10}^R with 0-dB coupling (if possible) and to suppress the unwanted propagating modes such as TE_{11}^C and TM_{11}^C by 40 dB across the 10.95–12.2- and 14.0–14.5-GHz frequency range. The superscripts C and R denote the circular and rectangular waveguides, respectively. To obtain 0-dB coupling between TE_{21}^C and TE_{10}^R, the cutoff frequencies in both the driven line and coupled line should be the same in order to obtain the same phase constant in the waveguides. Let A be the interior broadwall dimension of a rectangular waveguide and D be the inside diameter of a circular waveguide. To maintain the same cutoff frequency in both the rectangular and circular waveguides, it is found that

$$A = 0.51425D. \tag{11}$$

The cutoff frequency for the TE_{21}^C mode was chosen to be approximately 10 percent below the primary operating band at 11.7 GHz. Since 1.083-in diameter pipe was available for fabrication of breadboard couplers, this pipe was used, and the TE_{21}^C cutoff became 10.594 GHz. This cutoff also made it possible to have marginal performance at 10.95 GHz, which is only 3.4 percent above cutoff. Since coupling is a strong function of wall thickness and hole diameter, the actual waveguide wall thickness in the coupling region between the circular and the rectangular waveguides was chosen as 0.030 in.

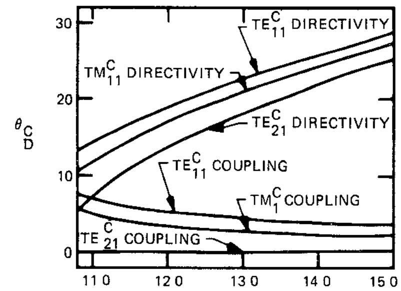

Fig. 6. θ_D^C versus frequency.

TABLE I
Values of τ for Modes of Interest

1	2	τ
TE_{21}^C	TE_{11}^C	0.36339
TE_{21}^C	TE_{21}^C	1 0
TM_{11}^C	TE_{21}^C	0 63517

A. Ku-Band Coupling Distribution

The phase constant in the waveguide can be expressed as

$$\beta = 2\pi\frac{f}{C}\sqrt{1-\left(\frac{f_C}{f}\right)^2}. \tag{12}$$

If we substitute (12) into (2), we obtain

$$\theta_D^C = L\frac{f}{C}\left[\sqrt{1-\left(\frac{f_{C1}}{f}\right)^2} \mp \sqrt{1-\tau\left(\frac{f_{C1}}{f}\right)^2}\right] \tag{13}$$

where

$$C = \text{velocity of light}$$

$$\tau = \left(\frac{f_{C2}}{f_{C1}}\right)^2 \leqslant 1.$$

The subscripts 1 and 2 denote the two modes to be investigated. By using the values of τ tabulated in Table I and a coupling length of 14.0 in (13), the variation of θ_D^C with operating frequency is generated. These curves are shown in Fig. 6. Based on these curves and the amplitude distribution of the electric field, the mode coupler can be designed.

In selecting a coupling distribution which would give an undesired mode rejection on the order of 40 dB, the work of Miller [1] was referred to extensively. He has shown that the worst rejection is obtained from uniform coupling distributions with various tapered distributions giving improved performance. Based on our examination of these distributions, it was found that the distribution that yielded the desired rejection in a minimum coupler length was the Bessel on a pedestal. This distribution gives −44-dB isolation of unwanted modes for a 48-hole distribution.

The optimum number of holes is a tradeoff between dimensional restrictions such as the spacing between holes,

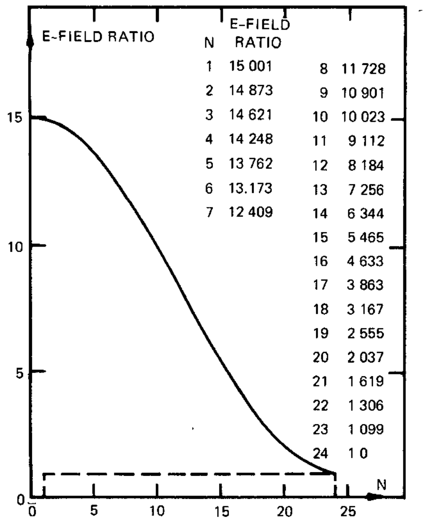

Fig. 7. Bessel function on a pedestal weighted coupling distribution.

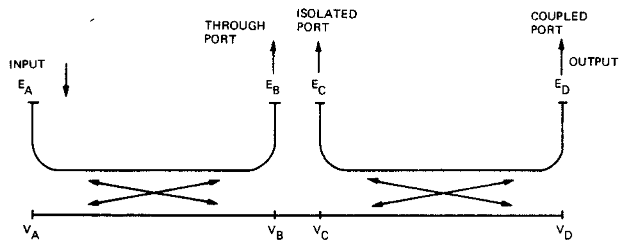

Fig. 8. Two identical couplers connected in series.

the maximum hole diameter, and the coupler length. Three sets of coupling holes were analytically investigated: 32, 48, and 64 holes. All three cases met the design requirements. By dimensional optimization between hole spacing and the maximum hole diameter, 48 holes were selected for the *Ku*-Band coupler design which is shown in Fig. 7.

B. One-Arm Coupler with Equal Holes

A convenient method to determine α_0 in (10) is from coupling measurements of a one-arm coupler with equal holes, since a_i is equal to 1 for all i for this case. Suppose two identical couplers are connected in series as shown in Fig. 8. Each coupler is symmetrical, equally spaced, and has equal coupling with $2N$ coupling points. Let E_A and E_D be the input and output, respectively, then the following equation is obtained:

$$\frac{E_D}{E_A} = \sin^2\left(2N\sin^{-1}\alpha_0\right). \tag{14}$$

The individual coupling per hole becomes

$$\alpha_0 = \sin\left[\frac{1}{2N}\sin^{-1}\left(\sqrt{\frac{E_D}{E_A}}\right)\right] \tag{15}$$

where the total coupling ratio E_D/E_A can be easily measured.

The individual hole coupling function α_0 is directly related to the waveguide coupling structure which can be rectangular, circular, or elliptical in shape. Circular holes were chosen since the circle is a simple geometry described by only one dimension D_0 (hole diameter). It has been shown that coupling is approximately expressed as a function of D_0^3 [1], [3], [4]. From curve fitting of measured data, an empirical expression for coupling was obtained and is given by

$$\alpha_0 = \left(3.002f^2 - 74.328f + 469.375\right)D_0^{3.6} \tag{16}$$

where f is the operating frequency in GHz.

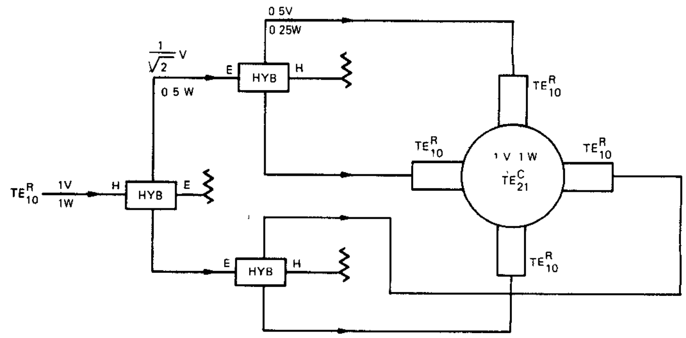

Fig. 9. Schematic diagram of comparator.

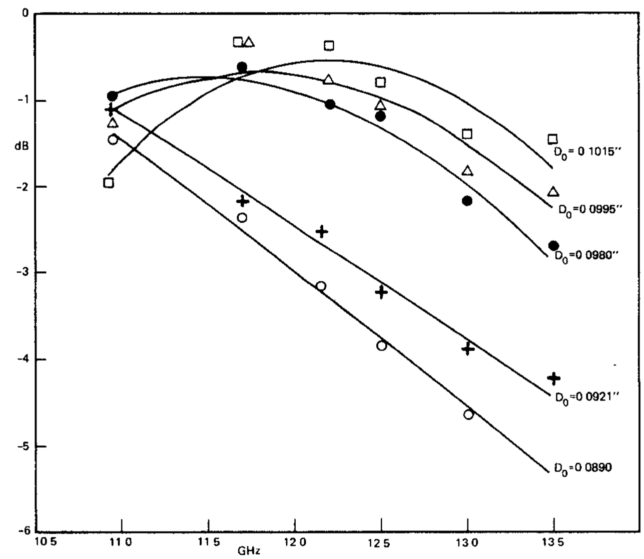

Fig. 10. Measured coupling as a function of frequency.

C. Four-Arm Coupler with Bessel Distributions

The four-arm coupler can be deduced from a one-arm coupler by including the comparator voltage division shown in Fig. 9. The four-ports should be transmission phase matched. The coupling ratio V_B/E_A (see Fig. 8) for the four-arm coupler can be expressed as

$$\frac{V_B}{E_A} = \sin\left[2\sum_{i=1}^{24}\sin^{-1}(2a_i\alpha_0)\right] \tag{17}$$

by neglecting loss terms. Since a_i is a known distribution shown in Fig. 7, we obtain $\alpha_0 = 0.002083$ by solving (17) for 0-dB coupling. Since α_0 is also expressed by (16), we obtain $D_0 = 0.0921$ in for 11.57 GHz.

Let d_i be the hole diameter ratio distribution corresponding to a_i, then d_i can be expressed as

$$d_i = a_i^{1/3.6} \tag{18}$$

while the actual hole diameter D_i is

$$D_i = D_0 d_i. \tag{19}$$

Successive coupling measurements were made using reference diameters (D_0) of 0.089, 0.0921, 0.098, 0.0995, and 0.1015 in. Fig. 10 shows the measured coupling data as a function of frequency. Minimum coupling loss for the 10.95–12.2-GHz frequency range was obtained for $D_0 =$ 0.098 in. The difference between the calculated optimum value of D_0 (0.0921 in) and the measured value of D_0 (0.098 in) is attributed to a change in sidearm phase constant caused by the perturbation that holes in the wall create. Therefore, measurement of the phase constant as a function of maximum hole diameter is necessary for accurate design. The best measured coupling of the TE_{21}-mode coupler described was -0.3 dB and is attributed due to dissipative loss of the coupler. Measured mode rejection between TE_{11}^C and TE_{21}^C modes is about 42-dB minimum from 10.95 to 14.5 GHz. Return loss of the TE_{11}^C mode in the through waveguide is about -30-dB maximum (1.065; 1 VSWR) from 10.95 to 20 GHz.

IV. Conclusion

A design procedure for a *Ku*-band TE_{21}-mode tracking couplers has been developed using mode-coupling theory. The coupler generates the TE_{21} mode without a phase shift since it is geometrically symmetric. This tracking (TE_{21}) mode does not interfere with the dominant (TE_{11}) mode due to more than 40-dB isolation between the two modes. This type of coupler makes wideband (25 percent bandwidth) tracking possible with coupling loss variation from 0.3 to 1.3 dB. Further measurements in our laboratory show that about 40 percent bandwidth with less than 2.0-dB coupling loss is possible. The VSWR of the coupler is less than 1.06 for about 80 percent bandwidth.

References

[1] S. E. Miller. "Coupled wave theory and waveguide applications," *Bell Syst. Tech. J.*, pp. 661–719, May 1954.

[2] S. E. Miller. "On solutions for two waves with periodic coupling," *Bell Syst. Tech. J.*, pp. 1801–1822, Oct. 1968.

[3] N. Marcuvitz. *Waveguide Handbook.* New York: McGraw-Hill, 1951, pp. 238–240.

[4] R. E. Collin. *Field Theory of Guided Waves.* New York: McGraw-Hill, 1960, pp. 285–307.

Youn H. Choung (S'76–M'79) was born in Seoul, Korea, on January 8, 1950. He received the B.S. degree from Yonsei University, Seoul, Korea, in 1972, and the M.S., and Ph.D. degrees from North Carolina State University, Raleigh, NC, in 1977 and 1979, respectively. He was a Research Assistant in the Electromagnetics Laboratory, North Carolina State University at Raleigh from 1975 to 1978. In 1978 he joined the Ford Aerospace and Communications Corporation, Palo Alto, CA. In the past, he has worked in the areas of Microwave Circuit Analysis and the Cavity Resonators in the Millimeter Waves. In most recent years, he has been involved with the development of both Spacecraft and Ground Microwave Antenna Systems such as the Monopulse Tracking Feed System, the Reuse Feed System, and the Optimization of the Multiple Beam Antenna Systems.

Dr. Choung is a member of Tau Beta Pi, Eta Kappa Nu and Pi Mu Epsilon.

Kenneth R. Goudey received the B.S.E.E. and M.S.E.E. degrees in 1966 and 1968, respectively, from San Jose State College, San Jose, CA.

He has been employed by Ford Aerospace and Communications Corporation for the past fourteen years in the design and development of communications antennas. He has written computer programs for analysis and synthesis of TEM lens antennas, Cassegrainian antennas, and Microwave components and feeds. As a Project Engineer, he has carried out a number of investigations in optimization of gain and noise temperature for ground-based antennas. As a Program Manager on the SOSI Program, he was responsible for the design and delivery of a high-power monopulse tracking feed for MIT Haystack radar. This feed was a multimode feed employing a multiflare horn for beam shaping. Mr. Goudey also designed, developed, and delivered a prime-focus feed and three-foot reflector for NASA-Houston to be used for simulation of Orbiter antenna operation using spread spectrum signals. He also designed and built an array simulator in waveguide for the purpose of studying the properties of frequency selective surfaces for implementation of multiple feeds in a single Cassegrain reflector system. He also designed and developed several extremely low axial ratio feed systems to be used in the frequency reuse communications networks. Several of these feed designs employ a polarizer design for which he currently holds a U.S. Patent.

Recently, Mr. Goudey has developed computer analysis programs to calculate the wide-angle radiation of multiple reflector antennas employing Geometric Theory of Diffraction and transform techniques to speed computation. He is also currently involved in development of EHF antenna systems operating in the 20 GHz to 50 GHz frequency range, and development of automated microwave measurement for improved accuracy and speed.

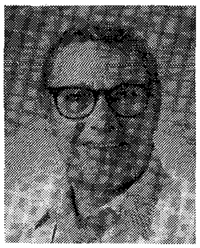

Lawrence G. Bryans (M'70) was born in Ames, Iowa in 1934. He received his A. B. degree in physics from California State University at Sacramento in 1959. He joined the corporation that was to become Ford Aerospace and Communications Corporation in 1959 where he has worked in the Western Development Laboratories Division. From 1959 to the present he has worked in the area of satellite communications antenna design. He is currently a Supervisor of the Microwave Engineering Section of the Antenna Engineering Department.

Mr. Bryans is a member of PGAP.